Biomedical Signal Processing and Control 52 (2019) 152–161

Contents lists available at ScienceDirect

Biomedical Signal Processing and Control

journal homepage: www.elsevier.com/locate/bspc

Synchrosqueezing transform based feature extraction from EEG signals for emotional state prediction

Pinar Ozel[a,*], Aydin Akan[b], Bulent Yilmaz[c]

[a] Electrical-Electronics Engineering Department, Nevsehir Hacı Bektas Veli University, Nevsehir, Turkey
[b] Biomedical Engineering Department, Izmir Katip Celebi University, İzmir, Turkey
[c] Electrical-Electronics Engineering Department, Abdullah Gul University, Kayseri, Turkey

ARTICLE INFO

Article history:
Received 27 April 2018
Received in revised form 11 March 2019
Accepted 14 April 2019
Available online 23 April 2019

Keywords:
Emotion recognition
Electroencephalography
Synchrosqueezing transform
Multivariate synchrosqueezing transform
VAD model

ABSTRACT

This paper presents a novel method for emotion recognition based on time-frequency analysis using multivariate synchrosqueezing transform (MSST) of multichannel electroencephalography (EEG) signals. With the advancements of the multichannel sensor applications, the need for multivariate algorithms has become obvious for extracting features that stem from multichannel dependency in addition to monochannel features. In order to model the joint oscillatory structure of these multichannel signals, MSST has recently been proposed. It uses the concepts of joint instantaneous frequency and bandwidth. Electrophysiological data processing mostly requires joint time-frequency analysis in addition to both time and frequency analysis separately. The short-time Fourier transform (STFT) and wavelet transform (WT) are the main approaches utilized in time-frequency analysis. In this paper, the feasibility and performance of multivariate wavelet-based synchrosqueezing algorithm was demonstrated on EEG signals obtained from publically available DEAP database by comparing with its univariate version. Eight emotional states were considered by combining arousal-valence and dominance dimensions. Using linear support vector machines (SVM) as a classifier, MSST and its univariate version resulted in the highest prediction accuracy rates of ϑ3% among all emotional states.

1. Background

New types of communication of humans with advanced media have the capability of reforming marketing [1], learning, gaming, *etc*. Multichannel electroencephalography (EEG) signals are used to communicate brain signals with the external systems and make interpretations about the state of emotions and intensions. Since emotions comprise an essential part in everyday life, the automatic emotion detection has been developed as a possible extension of brain computer interfaces (BCIs), which is a new human-machine communication approach. Emotion elicitation is possible from text, speech, facial expression or gesture. Lately, more studies have been carried out on emotion detection utilizing brain activities, especially EEG signals. Thanks to the new wireless headsets with features more suitable for consumers in terms of wearability, price, portability and ease-of-use, the EEG signals have recently been adopted in emotion detection which is the focus of this paper. We are concerned with the detection of ïnternalëmotions from EEG signals since facial expressions and vocal intonations may be controlled or manipulated in some way [2]. However, because of the nonstationarity of EEG signals, which is induced via convoluted neuronal movement in the brain, EEG signal analysis for emotion detection is a challenging research area. That is why advanced signal processing techniques are needed [3].

Emotion state categorization was proposed by Plutchik as eight essential emotional states, which are joy, sadness, anger, fear, disgust, surprise, anticipation, and acceptance [4]. Ekman et al. uncovered six fundamental emotions related with facial expressions which were surprise, sadness, happiness, disgust, fear, anger before enlarging the number of category of emotions by including shame, guilt, relief, satisfaction, sensory pleasure, contempt, contentment, embarrassment, amusement, pride in achievement [5]. The most broadly utilized arrangement is the bipolar model - valence and arousal dimensions- advocated by Russell [6,7] when it comes to the dimensional point of view. Valence corresponds to the nature of an emotion, ranging from disagreeable to wonderful. Arousal means the quantitative enactment level, from not excited to stimulated. Furthermore, pleasure-arousal-dominance (PAD) as a three-dimensional model was proposed by Mehrabian and Rus-

* Corresponding author at: Electrical-Electronics Engineering Department, Nevsehir Hacı Bektas Veli University, Nevsehir, Turkey.
E-mail address: pinarozel@nevsehir.edu.tr (P. Ozel).

https://doi.org/10.1016/j.bspc.2019.04.023
1746-8094/

sell in 1974 [2]. In addition to valence and arousal dimensions, the dominance dimension, which shows the control level of emotion, was included in this model (valence-arousal-dominance, VAD). It ranges from a sentiment being in control during sentimental experience to a sentiment of being controlled by the emotion [3,9]. With the assistance of the third emotional dimension, more emotional labels may be positioned in the three-dimensional space.

Although there are several studies in the literature dealing with the use of high/low arousal, high/low valence representation [4], and 2D valence-arousal space [5], there are limited number of studies in the literature where VAD space is used for emotional labeling. Liu and Sourina used VAD dimensions to recognize up to 8 emotions by utilizing a fractal dimension feature in combination with statistical and higher-order crossings (HOC) features [10–12,8,13]. Verma and his colleagues focused on, mostly, multimodal fusion framework to categorize and detect the emotions from physiological signals using multi-resolution approach by utilizing VAD model [14,15]. Walter et al. [16] evaluated a combined examination based on peripheral psychobiological measurements such as blood volume pulse (BVP), skin conductance level (SCL), and two-channel EMG to classify affective states. Wyczesany et al. demonstrated that 3D model was more consistent than the discrete model by utilizing independent components of brain activity derived from spontaneous EEG signals, and a mood self-report (PANAS-X) qualified on VAD space [17]. Guendil et al. contributed to VAD based literature by utilizing regularized extreme learning machine algorithm [18].

Emotion elicitation is typically considered as a classification problem where the decision of suitable features is significant to guarantee acceptable accuracy in terms of recognizing the emotion. An agreement on EEG-features to be used in emotion detection is not yet available. Both several time domain features such as different statistics, ERP, Hjorth features, fractal dimension, non-stationary index, higher order crossings and frequency domain features like signals in different frequency bands, band power, higher order spectra have been investigated by researchers in addition to time-frequency features such as discrete wavelet transform [19]. However, none of these studies focused on inter-channel dependencies that stem from multichannel data.

On the other hand, recent advances in time-frequency analysis area have prompted the improvement of high-resolution time-frequency algorithms, for example, the empirical mode decomposition (EMD) and the synchrosqueezing transform (SST) [20]. EMD is a method of decomposing a signal into its intrinsic mode functions [21]. This approach represents the signal as superposition of a small quantity of segments, each of which can be considered as harmonious locally, with moderate alterations of their amplitudes and frequencies. The nonlinear characteristic of the EMD method gives a conservative representation possibility. To some extent, however, the utilization of EMD for nonlinear signals has undermined some problems such as the so called “mode mixing” and “aliasing” problems [22]. Recently, EMD-based emotion detection strategies have been presented utilizing standard single and multiple channels of EEG signals [23–27]. In addition, multivariate empirical mode decomposition (MEMD) has lately been utilized in emotion recognition research [28,29,3,30,31]. Even though EMD has certain benefits for linear and non-stationary [21] data, its mathematical nature has not been well understood. The sensitivity of the EMD method to local signal alterations can frequently cause deteriorations. In any case, EMD approach tends to be m̈ode mixingẅhich stems from the overlaid intrinsic mode function (IMF) spectra and äliasingẅhich stems from the sub-Nyquist extreme sampling. Even though MEMD has certain favorable applications in dealing with multivariate non-stationary signals, it has a mode-mixing tendency [32].

Synchrosqueezing transform (SST), which is an EMD like approach, is proposed as a time-frequency analysis technique [20]. SST is a blend of wavelet decomposition and reassignment method, in addition to S-Transform [33] and Short-Time Fourier Transform (STFT) [34]. The aim of SST is to decompose the signals into some components with time-varying oscillatory features. This is achieved by reassigning the energies of STFT or continuous wavelet transform (CWT), or any similar time-frequency approach, such that the subsequent energies of coefficients are intense around the instantaneous frequency curves of the modulated oscillations. The frequency reassignment step of the procedure builds up the important localization of signal components in time-frequency domain [20]. Moreover, with the development of low-cost multichannel sensors, multivariate extensions of time-frequency algorithms are required to deal with inter-channel dependencies [35]. Thus, a compact time-frequency representation of multichannel signals has been generated based on the principles developed in [36–38] as a new time-frequency algorithm based on SST [20].

On the other hand, the modulated multivariate oscillation model based Multivariate Synchrosqueezing Transform (MSST) used in our study characterizes the compact representation of multivariate signals as a single oscillation structure that captures the attributes of the multivariable signal. In fact, the MSST algorithm divides the time-frequency domain into sections to define a series of modulated oscillations that are common to the data channels in the multivariate data, inspired by the MEMD algorithm. Considering a multivariate extension of the SST algorithm, a multivariate time-frequency representation is developed in which modulated multivariate oscillations are defined [35].

The purpose of this study is to demonstrate a 3D valence-arousal-dominance model based emotional state prediction by processing of multichannel EEG signals. Moreover, our aim is to present new options for more reliable classification results utilizing SST and MSST methods that have recently been proposed in the area of time-frequency representations. Furthermore, to investigate the advantages of taking multichannel dependencies into account, SST is applied on the EEG channels individually, and MSST is applied on all the channels simultaneously for emotional state classification, and their results are compared.

2. Materials and methods

2.1. Synchrosqueezing transform

Synchrosqueezing transform, which is a post-processing procedure based on continuous wavelet transform (CWT) in general, is a strategy intended to concentrate the oscillation components of a signal and to acquire localized time-frequency (TF) representations of non-stationary signals.

The general form of the signal $x(t)$ is specified in the following form.

$$x(t) = \sum_{n=1}^{N} x_n(t) + e(t) \tag{1}$$

where each component $x_n(t) = A_n(t)\cos(\emptyset_n(t))$ is an oscillation function, with time-varying amplitude and frequency, and $e(t)$ denotes the noise. The aim here is to obtain the amplitude $A_n(t)$ and the instantaneous phase $\emptyset_n(t)$ for each component, $n = 1,\ldots N$. After applying the Hilbert Transform to the original $x_n(t)$ component, the analytic signal $p_n(t)$ is formed as

$$p_n(t) = A_n(t)\, e^{j\Phi n(t)} = x_n(t) + i\mathrm{H}\left\{x_n(t)\right\} \tag{2}$$

Extending $p_n(t)$ for the multicomponent signal by constructing a vector consisting of each channel's analytical signal, multivariate analytic signal is obtained as:

$$p_n(t) = \begin{bmatrix} A_1(t)e^{j\Phi_1(t)} \\ A_2(t)e^{j\Phi_2(t)} \\ A_3(t)e^{j\Phi_3(t)} \\ A_4(t)e^{j\Phi_4(t)} \\ \vdots \\ \vdots \\ A_N(t)e^{j\Phi_N(t)} \end{bmatrix} \quad (3)$$

Therefore, each EEG channel is a monocomponent signal as in Eq. (3). In the SST algorithm, a highly localized time-frequency representation for the multicomponent signal $x(t)$ is obtained using the instantaneous amplitude and frequency information extracted from the above analytic signal by employing the CWT.

The CWT algorithm perceives oscillatory components of a signal utilizing time-frequency filters known as wavelets. The mother wavelet ψ(t) is the finite oscillation function that is convolved with the signal x(t). CWT of $x_n(t)$ is calculated as follows:

$$W(a,b) = \int a^{-\frac{1}{2}} \Psi\left(\frac{t-b}{a}\right) x_n(t)dt \quad (4)$$

Here, $W(a, b)$ represents the wavelet coefficients for each scale-time pair (a, b). As such, the wavelet coefficients may be seen as the outputs of a band-pass filter. The scale factor 'a' scrolls the band-pass filter in the frequency domain and changes the bandwidth of the filter. The frequency properties relies upon the scale parameter a, where the shift parameter 'b' represents the time of interest. Thus, at the frequency of w_s, the energy of a sinusoidal wavelet transform is spread around the scale factor $a_s = {}^{w_\Psi}/_{w_s}$. Here, w_Ψ is the center frequency of a wavelet, while the energy of the original frequency w_s is spread across a_s. Accordingly, the original frequency w_r and the estimated frequency in those scales are the same. Therefore, for each scale-time pair (a, b), the instantaneous frequency $w_x(a, b)$ can be evaluated as:

$$w_x(a,b) = -iW(a,b)^{-1}\frac{\partial W(a,b)}{\partial b} \quad (5)$$

The SST method transforms the wavelet coefficients from the scale-time domain to the time-frequency domain. As such, every point (a, b) is transformed into $(b, w_x(a, b))$. Since a and b are discrete values, we need a scaling step. $\Delta a_k = a_{k-1} - a_k$ for any a_k where $w_x(a, b)$ is calculated. During the time-scale to time-frequency domain transformation, $(b, a) \rightarrow (b, w_{inst}(a, b))$, the SST coefficient $T(w_l, b)$ is computed only at the centers w_l of the frequency range $(w_l - \frac{\Delta w}{2}, w_l + \frac{\Delta w}{2})$ with $\Delta w = w_l - w_{l-1}$. Here, w_l is the frequency bins at a resolution of Δw. Here, Δw shows linear frequency scales, so it is a constant value. The SST reconstructs the oscillations in the univariate module of $x_n(t) = A_n(t)\cos(\emptyset_n(t))$. So, the synchrosqueezing coefficient and reconstructed signal $x(b)$ are given below:

$$T(w_l,b) = \sum_{a_k:|w_x(a_k,b)-w_l|\le\Delta w/2} W(a_k,b)a^{-3/2}\Delta a_k \quad (6)$$

$$x(b) = \Re\left[R_\Psi^{-1}T(w_l,b)\Delta\omega\right] \quad (7)$$

Eq. (4) demonstrates that the TF representation of the signal is synchrosqueezed along the frequency scale. In Eq. (7), $R_\Psi = \frac{1}{2}\int_0^\infty \tilde{\Psi}^*(\xi)\frac{d\xi}{\xi}$ is the normalization constant and $\hat{\Psi}(\xi)$ is the Fourier Transform of the mother wavelet $\Psi(t)$. In the SST algorithm, the coefficients of the CWT are reallocated to handle a consistent representation over the time-frequency domain, from which the instantaneous frequencies are subsequently generated

2.2. Multivariate synchrosqueezing transform

As shown above, the modulated oscillation model, which provides improvement of modern time-frequency algorithms, gives an expressive representation in the time-frequency domain. To recognize oscillations common to multiple data channels, this concept is expanded for multivariate signals by presenting a multivariate extension of the synchrosqueezing transform thanks to the idea of joint instantaneous frequency multivariate data [35]. Given a multivariate data like EEG, the process starts by applying SST to all channels. At this step, synchrosqueezing coefficients are obtained for all channels. After this point, the rules of multichannel dependency of the modulated oscillation model is employed. In order to identify a set of mono-component signals from a given multivariate signal, the time-frequency domain is separated into K frequency bands $\{w_k\}_{k=1,\ldots K}$. Then, the instantaneous amplitudes and frequencies exist within these frequencies are determined. With respect to the most significant step, by computing the joint instantaneous frequency of each oscillatory scale across the channels, multivariate instantaneous frequency and instantaneous amplitude are calculated, respectively. Finally, the multivariate synchrosqueezing coefficient is determined by utilizing multivariate instantaneous frequency and instantaneous amplitude.

2.2.1. Multivariate bandwidth estimation

The partition of the time frequency domain in multivariate synchrosqueezing transform depends on multivariate bandwidth. Multivariate Bandwidth estimates the bandwidth in a determined each frequency scale, for all the channels.

It should be noted that multivariate bandwidth utilizes the concept of the joint instantaneous frequency known as the power weighted average of the instantaneous frequency of all the channels and the joint instantaneous bandwidth representing the normalized error of the joint instantaneous frequency estimate with respect to the rate of change of the multivariate analytic signal $p_n(t)$ Accordingly:

- The joint instantaneous frequency catches the consolidated oscillatory elements of the multivariate signals presented as:

$$\omega_p(t) = \frac{\zeta\left\{p_n^H(t)\,dtp_n(t)\right\}}{||p_n(t)||^2} = \frac{\sum_{n=1}^{N} A_n^2(t)\dot{\phi_n}(t)}{\sum_{n=1}^{N} A_n^2(t)} \quad (8)$$

Here, the symbol "$\dot{\phi_n}(t)$" represents the instantaneous frequency for each channel and "" represents the imaginary part of the complex signal.

- The joint instantaneous bandwidth catches the deviations of the multivariate oscillations for each channel utilizing the joint instantaneous frequency presented as:

$$v_p(t) = \frac{||\frac{d}{dt}p_n(t) - i\omega_p(t)p_n(t)||}{||p_n(t)||} \quad (9)$$

- Attaching the Eqs. (3) into (9) comes out the statement of the squared instantaneous bandwidth as:

$$v_p^2(t) = \frac{\sum_{n=1}^{N} A_n'(t))^2 + \sum_{n=1}^{N} A_n^2(t)(\emptyset_n'(t) - \omega_p(t))^2}{\sum_{n=1}^{N} A_n^2(t)} \quad (10)$$

Therefore, the global moments of the joint analytic spectrum can be stated through the joint instantaneous frequency and bandwidth. The first and second global moments are entitled the joint mean frequency and the joint global second central moments (multivariate bandwidth squared). Hereby, the joint analytic spectrum is given as:

$$S(\omega) = \frac{1}{E} | \left| P_n(\omega) \right| |^2 \quad (11)$$

Here, $P_n(\omega)$ is the Fourier Transform of $p_n(t)$ and the E is the total energy of the frequency domain calculated as:

$$E = \frac{1}{2\pi} \int_0^{\infty} | \left| P_n(\omega) \right| |^2 d\omega \quad (12)$$

The joint analytic spectrum and the total energy make possible to describe the joint global mean frequency stated as the first moment of the joint analytic spectrum as follows:

$$\bar{\omega} = \frac{1}{2\pi} \int_0^{\infty} \omega S(\omega) d\omega \quad (13)$$

The joint global second central moment (the multivariate bandwidth squared) evaluates the spectral deviations of the joint analytic spectrum from the joint global mean frequency, and presented as:

$$\bar{\sigma}^2 = \frac{1}{2\pi} \int_0^{\infty} (\omega - \bar{\omega})^2 S(\omega) d\omega \quad (14)$$

Therefore, the global moments of the analytic spectrum can be identified with the moments of joint instantaneous frequency and bandwidth given as:

$$\bar{\omega} = \frac{1}{E} \int_{-\infty}^{\infty} \left| \left| p_n(t) \right| \right|^2 \omega_p(t) dt \quad (15)$$

$$\bar{\sigma}^2 = \frac{1}{E} \int_{-\infty}^{\infty} \left| \left| p_n(t) \right| \right|^2 \sigma_p^2(t) dt \quad (16)$$

Here, $\sigma_p^2(t)$ is the joint instantaneous second central moment (the multivariate bandwidth squared), presented as follows:

$$\sigma_p^2(t) = v_p^2(t) + (\omega_p(t) - \bar{\omega})^2 \quad (17)$$

The multivariate bandwidth squared, σ^2, relies upon both the joint instantaneous bandwidth, $\sigma_p^2(t)$, and the deviations of the joint instantaneous frequency from the joint global mean frequency, $\bar{\omega}$.

As a start, time-frequency domain is sliced into 2^l frequency bands with equal width on the account of the frequency range as $w_{l,m} = \left[\frac{m}{2^{(l+1)}}, \frac{(m+1)}{2^{(l+1)}}\right]$ where $l = 0, \ldots, L$ represents the levels of the frequency bands (default value as $L = 5$) and $m = 0, \ldots 2^l - 1$ denotes the index for the frequency band. From this point, the multivariate bandwidth is estimated for each band, then, the step of the estimation the bandwidth with power of the signal accounted for is evaluated. After splitting the frequency bin as it is shown in Fig. 1, the lowest frequency band is splitted if power level is higher then the other frequency bands. Therefore, the multivariate bandwidth $B_{l,m}$ within a given frequency band $w_{l,m}$ is divided into the frequency sub-bands $w_{l+1,2m}$ and $w_{l+1,2m+1}$.

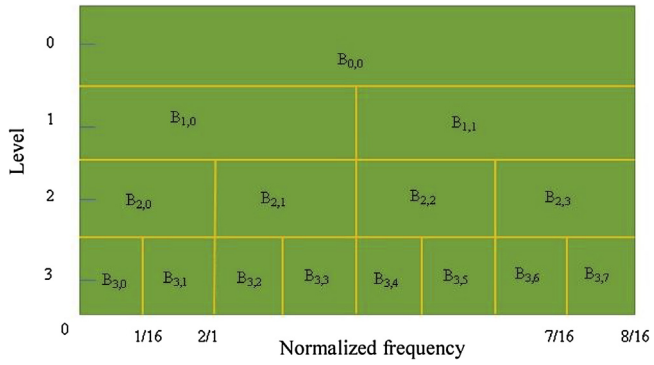

Fig. 1. The sectioned frequency domain with the multivariate bandwidth presented by $B_{l,m}$ where l shows the level of the frequency band and m is the frequency band index.

1 As such, for a given multichannel signal $x_n(t)$ with N channels, SST is applied to each channel to obtain $T_n(w, b)$ coefficients.
2 Then the SST coefficient for each channel $T_n(w,b)$ is normalized with the normalization constant, and a given set of oscillatory scales $\{w_k\}_{k=1,\ldots K}$., for the time-frequency representation, a series of sections along the frequency axis are determined, the instantaneous frequency $\Omega_k^n(b)$ and the instantaneous amplitude $A_k^n(b)$ for each frequency section are calculated.

$$\Omega_k^n(b) = \frac{\sum_{w \varepsilon w_k} \left| T_n(w, b) \right|^2 w}{\sum_{w \varepsilon w_k} \left| T_n(w, b) \right|^2} \quad (18)$$

$$\mathrm{A_k^n(b)} = \sqrt{\sum_{\mathrm{w \varepsilon w_k}} |\mathrm{T_{n(w,b)}}|^2} \quad (19)$$

3 Multivariate instantaneous frequency $\Omega_{\mathrm{k}}^{\mathrm{multi}}(\mathrm{b})$ and instantaneous amplitude $\mathrm{A_k^{multi}(b)}$ are calculated, respectively.

$$\omega_k^{multi}(b) = \frac{\sum_{n=1}^{N} \left(A_k^n(b)\right)^2 \omega_k^n(b)}{\sum_{n=1}^{N} \left(A_k^n(b)\right)^2} \quad (20)$$

$$A_k^{multi}(b) = \sqrt{\sum_{n=1}^{N} \left(A_k^n(b)\right)^2} \quad (21)$$

4 The multivariate synchrosqueezing coefficient $T^{multi}(w,b)$ is determined [35].

Now that the joint instantaneous amplitude and frequency for each frequency band are calculated, the multivariate time-frequency coefficients $T_k{}^{multi}(w,b)$ for each oscillatory scale k is obtained as follows:

$$\mathrm{T_k^{multi}(w, b)} = \mathrm{A_k^{multi}}\ \delta(w - \Omega_k^{multi}(b)) \quad (22)$$

Here, $\delta(.)$ is the Dirac delta function, and the multivariate time-frequency coefficients for each oscillatory scale are denoted by $T^{multi}(w,b) = T_k{}^{multi}(w,b)|_{k=1,\ldots K}$. It is essential to note that since the phase information is lost during the instantaneous frequency computation, the signal $\mathrm{x_n(t)}$ may not be reconstructed.

2.3. Dataset

DEAP "(*A Dataset for Emotion Analysis and using EEG, Physiological and video signals)*" dataset [39] is a database, which is available to conduct academic research with permission, includes collection of EEG signals from various participants for emotion study. Specifically, the subjects watched music videos to incite different feelings and evaluated every video with respect to arousal, valence, like/dislike, dominance, and familiarity parameters, completing self-assessment manikins (SAM) and evaluated with the scale of 1 to 9 for emotional statements at the end of each video clip. The database is comprised of multichannel EEG signals from 32 subjects (16 men and 16 women, whose ages range from 19 to 37, and mean age 26.9). Before the session started, a two-minute long EEG signal was acquired while viewing a fixation cross on the screen. The EEG signals were recorded using international 10–20 positioning system [40] and a sampling frequency of 512 Hz.

The recordings were the same for all subjects yet sequence of visualization for each participant was random. In our study, valence, arousal and dominance dimensions were evaluated. The data was provided by [39] in the preprocessed form in which the recordings were down-sampled to 128 Hz, EOG artifacts were removed, and a band-pass filter with cutoff frequencies of 4.0–45.0 Hz was used.

2.4. Classification

2.4.1. K-nearest neighborhood classification

One of the simplest decision procedures that can be used for classification is the nearest neighbor rule. It classifies a sample according to the category of the nearest neighbor. The closest neighboring classifiers are based on learning by comparing test identification groups with training identification groups similar to it. When not familiar with an identification group, then the k-nearest neighbor classifier searches for the sample gap for the training data that is closest to the unknown identification group. These training identification groups are the c̈losest neighborsöf unknown identification groups. Proximity was defined using Euclidean distance [41].

2.4.2. Decision tree

Decision trees are popular machine learning classification methods, because they provide easy-to-understand information models. Discrimination is generally made between methods that use continuous variables rather than discrete, categorical variables. The classification is carried out using a tree structure that divides the input field based on sample data by classifying individuals from the base in the r̈ootänd l̈eafn̈odes. Starting from the root (for example, a mixture of individuals from different populations), each node in the tree contains a test question about a single variable (or property). The critical step in the decision tree is to specify which feature is tested on each node. This decision is initially calculated by the entropy defined as the entropy of each variable [42–44].

2.4.3. Ensemble classifiers

Ensemble models are widely used in many areas because they are more stable and, more importantly, they are considered to be better than singular classifiers. It is also known to reduce model bias and variance. Ensemble classifiers collect estimates of more than one basic model. Many empirical and theoretical evidence showed that the combination of models increases predicted accuracy. Ensemble students create basic models in an independent or dependent manner. To avoid errors in existing ensemble, re-trained basic models are added [45–47].

2.4.4. Support vector machine

Support Vector Machines categorize data via determination of an arrangement of support vectors, minimizing the Structural Risk. The support vectors are insiders of an arrangement of training inputs that sketch a hyperplane in feature space. This k-dimensional hyperplane in which k is the quantity of features of the input vectors, describes the boundary among the distinct classes. The mission in the classification is essentially to determine which side of the hyperplane the testing vectors exist in. Underrating the structural risk diminish the average error of the inputs and their target vectors. The training data are categorized into binary classes [48,49].

2.5. Methodology

2.5.1. Channel selection

In recent years, time domain, frequency domain, joint time-frequency domain techniques, non-standardized channels, and feature selection studies have suggested that emotion modeling is a controversial issue. Specifically, the use of different dataset and different channels makes it difficult to compare method performances between dataset groups and channels. Given the emotional state analysis, channel selection is an important problem since all parts of the brain do not function in emotion recognition. Channels located on the frontal lobe are used in emotional state analysis studies. However, there are also studies using only one of the channels or selected channels in their preferred channel arrangement.

Considering the feature selection algorithms for channel selection in emotional modelling, [50,19,51–56] have proposed different feature selection approach for channel contribution. However, channel preferences for emotion recognition are also based on neuroscientific information, rather than feature selection methods for the EEG channels. Based on neuroscience, the selected channel studies mostly do not include the same channel groups by applying the feature selection with studies according to the selected channel.

On the other hand, there are studies in literature using symmetric electrode pairs. From these studies, in addition to obtaining power spectral attributes from 32 channels in the DEAP dataset, the differences between the spectral power of all symmetrical electrode pairs in the right and left hemisphere were also utilized to measure the possible asymmetry in brain activities associated with emotional stimuli for the 14 electrode pairs [39]. In the work of [57] they benefited from the concept of differential asymmetry index by taking the channel difference in order to obtain the predictive attributes for each of the seven symmetric channel pairs. In addition [58,59,3], and [60] have used the difference in the electrode pair.

Therefore, in this study, the right frontal weight of the lobe (Fp2, AF4, F4, F8, FC2, FC6, T8, C4) and the left weighted frontal lobe (Fp1, AF3, F3, F7, FC1, FC5, T7, C3), right and left frontal weight lobe differences (Fp1-Fp2, AF3-AF4, F3-F4, F7-F8, FC1-FC2, FC5-FC6, T7-T8, C3-C4) and 2 central channels (Fz, Cz) was the input data as a total of 26 channel EEG signal input. EEG channels in this region are used in emotional state analysis studies due to the presence of the affective area in the frontal lobe of the brain.

2.5.2. Assignments for valence –arousal-dominance labels

For valence and arousal scores given by the subjects, a thresholding is applied such that the values varying from 1 to 9 are labeled as Low (less than 5) or High (greater than 5), and the dominance values were set to 0 or 1. If both valence and arousal labels were high, positive valence high arousal "PVHA" label, if valence was low and arousal was high, negative valence high arousal "NVHA" label is assigned. Similarly, positive valence low arousal "PVLA", and negative valence low arousal "NVLA" labels were assigned. Furthermore, after assigning these labels to four emotional states, the contribution of dominance label was considered. For each of the above emo-

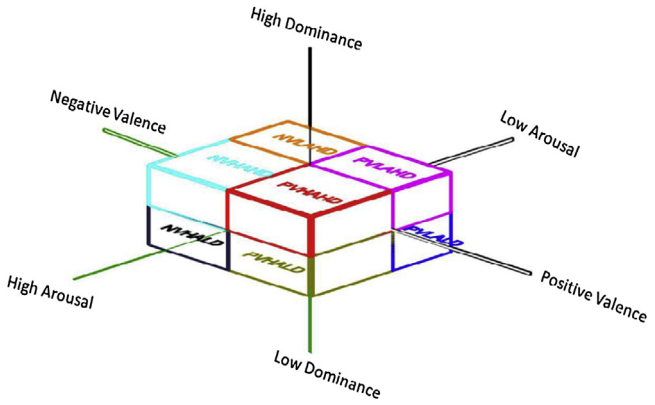

Fig. 2. Eight emotional states representation in VAD model (Front view of emotional states in spatial plane).

tions, if the dominance label is equal to 1, ". . ..HD", if it is 0, ". . ..LD" labels are generated comprising "PVHAHD", "PVHALD", "NVHAHD", "NVHALD", "PVLAHD", "PVLALD", "NVLAHD", "NVLALD" labels for eight emotional states. Therefore, from the database we acquire PVHAHD:378, PVHALD:66, PVLALD:173, PVLAHD:125, NVHAHD:191, NVLALD:188, NVLAHD:86, NVHALD: 101. Eight emotional state representation in VAD model are presented in Fig. 2.

2.5.3. MSST and SST features from the EEG data

EEG signals of 32 subjects and 40 video recordings given in the DEAP dataset were considered. For each subject a total of 26 channels, the right frontal-weighted lobe (Fp2, AF4, F4, F8, FC2, FC6, T8, C4), the left frontal-weighted lobe (Fp1, AF3, F3, F7, FC1, FC5, T7, C3), right and left frontal-weighted lobe differences as virtual channels and 2 central channels (Fz, Cz), were used in the analysis. From each 1-minute long recording, the first 4032 samples were analyzed, thus a three-dimensional dataset of size $26 \times 40 \times 4032$ were constructed for further processing for each subject. The MSST coefficients were computed for each one of the 40 video recordings, forming a $26 \times 2017 \times 4032$ matrix. Singular value decomposition (SVD) is applied to the data for dimension reduction yielding a $52{,}442 \times 1$ vector. Considering 32 subjects times 40 videos, an input matrix of $1280 \times 52{,}442$ was formed. Classification of the extracted EEG features was performed using MATLAB Classification Learner Tool and the classification performances were evaluated. 10-fold cross validation is used in the performance evaluation (Fig. 3).

Additionally, to investigate the advantages of considering multichannel dependencies in our EEG signals, we applied the SST algorithm to 26 channels separately for 40 videos of 32 subjects. Calculated SST features are used for the classification using the same classifiers and performances of MSST and SST features based approaches are compared.

3. Results

In this study, we utilized both SST and MSST algorithms for feature extraction to show their performances on our data for emotion classification using both 2D and 3D emotion models.

1) In our first experiments, we applied 2D valence-arousal model to estimate four emotional states using MSST features and various decision trees, SVMs, kNNs, and ensemble classifiers at the classification stage. Table 1 shows the classification accuracies for all emotions and classifiers where the best classification performances were obtained for coarse kNN, Gaussian SVM, and boosted trees with 79.1% classification accuracies. Quadratic and cubic SVM, and RUSBoosted trees approaches performed poorly.
2) We then applied 3D valence-arousal-dominance (VAD) model to estimate eight emotional states by using MSST features and the same classifiers used above. The accuracy levels reached 93% for several emotions, as shown in Table 2. Even though there are more emotional states in the classification problem, accuracies are higher for eight state model than that of the four state model.
3) Finally, we applied the SST method to each one of the 26 EEG channels separately to estimate the eight emotional states in

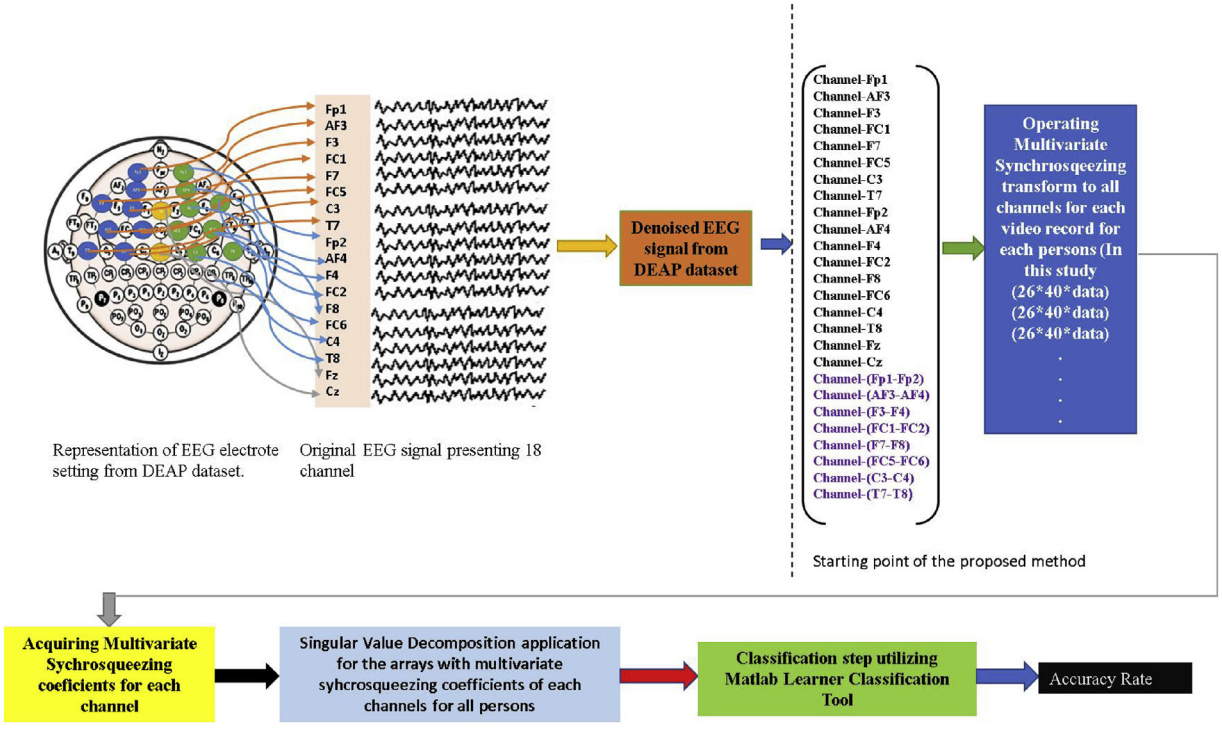

Fig. 3. Steps of the proposed method.

Table 1
Classification results of four emotional states in 2D valence-arousal model utilizing MSST features. The classification performances are shown as percentage accuracy.

Classification Methods	PVHA	NVHA	PVLA	NVLA	Avg.Acc.%
DECISION TREES					
Complex Tree	60.5	**69.5**	67.5	69.1	66.65
Medium Tree	69.1	**76.3**	73.4	74.5	73.33
Simple Tree	69.8	**78.6**	76.8	77.7	**75.73**
Average	66.47	**74.80**	72.57	73.77	
SUPPORT VECTOR MACHINE					
Linear SVM	68.4	**78.7**	76.7	78.0	75.45
Quadratic SVM	61.1	**62.5**	41.6	46.6	52.95
Cubic SVM	43.7	55.9	**61.4**	44.8	51.45
Fine Gaussian SVM	70.7	**79.1**	77.1	78.2	76.28
Medium Gaussian SVM	70.8	**79.1**	77.1	78.2	76.30
Coarse Gaussian SVM	70.8	**79.1**	77.1	78.2	**76.30**
Average	64.25	**72.4**	68.5	67.33	
NEAREST NEIGHBOR CLASSIFIERS					
Fine kNN	58.0	**68.4**	63.8	66.4	64.15
Medium kNN	69.8	78.5	76.6	**77.3**	75.55
Coarse kNN	70.7	**79.1**	77.1	78.2	**76.28**
Cosine kNN	68.8	**78.4**	76.4	78.1	75.43
Cubic kNN	70.2	**78.0**	76.2	77.4	75.45
Weighted kNN	65.2	**74.9**	72.3	73.9	71.58
Average	67.12	**76.22**	73.73	75.22	
ENSEMBLE CLASSIFIERS					
Boosted Trees	70.9	**79.1**	77.1	78.2	**76.33**
Bagged Trees	66.5	**75.5**	74.1	75.1	72.80
Subspace Discriminant	62.8	**69.1**	68.1	67.5	66.88
Subspace kNN	61.1	69.1	66.4	**70.5**	66.78
RUSBoosted Trees	**70.2**	45.8	37.8	38.2	48.00
Average	66.3	**67.72**	64.7	65.9	

3D VAD model and give the results in Table 3. Comparing these results with Table 2, we observe that the classification performances of quadratic and cubic SVM, and RUSBoosted trees increased significantly for individual application of SST on each channel. The same classifiers yielded the highest accuracy values compared to other classifiers. The classification accuracies are the highest for NVLAHD and NVHALD emotional states, and lowest for PVHAHD state consistently.

3.1. Analysis of the classifiers performance

In the classification part of our study, support vector machines (SVM), decision tree (DT), nearest neighbor classifier (NNC), and ensemble classifier (EC) approaches available in MATLAB Classification Learner Tool are used. The SVM approach turns the classification problem into a quadratic optimization problem, and choice of kernel function and parameter optimization are critical part of the algorithm. Speed of SVM algorithm was low. Memory requirement was medium for linear SVM, but for other kernels it was high for binary type classes and medium for multiclass [61]. The DT approach is built from top to bottom more than once dividing and conquering. The classification speed was high, and the memory usage was low [62]. As for the NNC, we utilized *k*-NN algorithm which is an unsupervised and basic classification method. The operating speed was medium except for the cubic k-NN, which was slow. Furthermore, memory usage was medium [41]. The performance of EC is based on two fundamental criteria: *i)* the success of main classifiers inside the ensemble, and *ii)* the distinction of the choices of essential learners. Thus, estimation speed ranged from rapid to medium according to the selection of the parameters. Memory usage ranged from low to high as indicated by the choice of the main classifiers [45].

4. Discussion

This study investigates the feasibility of SST and MSST approaches, which are recently developed time-frequency analy-

Table 2
Classification results of eight emotional states in 3D valence-arousal-dominance model utilizing MSST features. The classification performances are shown percentage accuracy.

Classification Methods	PVHAHD PVHAHD PP	PVHALD	PVLALD	PVLAHD	NVLALD	NVHALD	NVHAHD	NVLAHD	Avg.Acc.% Accuracyy
DECISION TREES									
Complex Tree	63.7	84.2	77.4	81.3	77.3	85.7	74.1	**88.2**	78.99
Medium Tree	71.2	86.9	84.5	87.3	83.0	89.9	83.5	**91.5**	84.73
Simple Tree	74.0	88.6	86.5	89.6	84.7	91.6	84.8	**92.7**	**86.56**
Average	69.6	86.57	82.80	86.07	81.67	89.07	80.80	**90.80**	
SUPPORT VECTOR MACHINES									
Linear SVM	65.9	88.1	86.3	89.8	85.4	91.6	84.5	**93.0**	85.58
Quadratic SVM	68.4	44.5	**76.8**	30.7	66.6	74.5	51.0	70.9	60.43
Cubic SVM	45.2	**61.8**	45.9	51.2	27.4	16.8	43.4	12.0	37.96
Fine Gaussian SVM	73.4	88.8	86.5	90.2	85.3	**92.1**	85.1	93.3	86.84
Medium Gaussian SVM	73.9	88.8	86.5	90.2	85.3	**92.1**	85.1	93.3	**86.90**
Coarse Gaussian SVM	73.7	88.8	86.5	90.2	85.3	**92.1**	85.1	93.3	86.88
Average	66.7	76.80	**78.08**	73.72	72.55	76.53	72.37	75.97	
NEAREST NEIGHBOR CLASSIFIERS									
Fine kNN	61.3	84.6	76.8	81.3	75.9	86.9	76.0	**87.9**	78.84
Medium kNN	71.5	88.8	86.4	90.2	85.2	92.1	84.8	**93.3**	86.54
Coarse kNN	74.0	88.8	86.5	90.2	85.3	92.1	85.1	**93.3**	**86.91**
Cosine kNN	72.0	88.8	86.5	90.2	85.2	92.1	85.1	**93.3**	86.65
Cubic kNN	71.4	88.8	86.3	90.2	85.2	92.1	84.9	**93.3**	86.53
Weighted kNN	68.2	88.2	84.1	89.0	83.9	91.1	82.3	**92.9**	84.96
Average	69.7	88.00	84.43	88.52	83.45	91.07	83.03	**92.33**	
ENSEMBLE CLASSIFIERS									
Boosted Trees	74.1	88.8	86.5	90.2	85.3	92.1	85.1	**93.3**	**86.93**
Bagged Trees	68.3	88.2	85.2	89.6	84.5	91.5	83.8	**93.0**	85.51
Subspace Discriminant	67.7	85.3	78.8	84.2	77.3	87.2	77.3	**88.5**	80.79
Subspace kNN	64.1	86.0	79.8	84.7	79.8	87.7	78.0	**90.6**	81.34
RUSBoosted Trees	**73.3**	72.9	29.2	33.9	37.5	37.5	60.9	33.2	47.30
Average	69.5	**84.24**	71.9	76.52	72.88	79.2	77.02	79.72	

Table 3
Classification results of eight emotional states in 3D valence-arousal-dominance model utilizing SST features for each channel separately. The classification performances are shown as percentage accuracy.

Classification Methods	PVHAHD	PVHALD	PVLALD	PVLAHD	NVLALD	NVHALD	NVHAHD	NVLAHD	Avg.Acc.%
DECISION TREES									
Complex Tree	69.6	85.1	82.7	84.7	76.6	86.3	77.0	**88.2**	81.27
Medium Tree	73.2	86.1	85.6	87.8	81.6	89.1	82.6	**89.9**	84.48
Simple Tree	70.8	87.8	86.7	89.3	84.4	90.8	84.2	**92.4**	**85.80**
Average	71.2	86.33	85.00	87.27	80.87	88.73	81.27	**90.17**	
SUPPORT VECTOR MACHINE									
Linear SVM	72.6	88.8	86.5	90.2	85.3	92.1	85.1	**93.3**	86.74
Quadratic SVM	74.1	88.5	84.7	87.3	81.8	**90.9**	80.9	90.5	84.84
Cubic SVM	70.0	87.0	82.3	86.6	79.8	89.4	79.3	**89.8**	83.03
Fine Gaussian SVM	75.7	89.8	86.5	90.2	85.2	92.1	85.1	**93.3**	**87.24**
Medium Gaussian SVM	71.3	89.8	86.5	90.2	85.3	92.1	85.1	**93.3**	86.70
Coarse Gaussian SVM	70.5	89.8	86.5	90.2	85.3	92.1	85.1	**93.3**	86.60
Average	72.3	88.9	85.50	89.12	83.78	91.45	83.43	**92.25**	
NEAREST NEIGHBOR CLASSIFIERS									
Fine kNN	67.6	**86.7**	82.4	81.9	77.5	85.9	77.3	85.2	80.56
Medium kNN	74.5	88.8	86.6	90.2	85.2	92.1	84.1	**93.3**	86.85
Coarse kNN	72.7	88.8	86.5	90.2	85.3	92.1	85.1	**93.3**	86.75
Cosine kNN	74.2	88.8	86.3	90.2	85.3	92.1	84.4	**93.3**	**86.83**
Cubic kNN	74.6	88.3	86.2	90.2	85.3	92.0	84.5	**93.3**	86.80
Weighted kNN	73.4	88.4	85.8	88.2	82.3	90.9	83.4	**92.0**	85.55
Average	72.8	88.30	85.63	88.48	83.48	90.85	83.13	**91.73**	
ENSEMBLE CLASSIFIERS									
Boosted Trees	70.5	88.8	86.5	90.2	85.2	92.1	85.1	**93.3**	**86.46**
Bagged Trees	72.9	87.9	85.4	87.7	82.0	90.7	81.5	**92.0**	85.01
Subspace Discriminant	73.1	86.2	84.0	85.9	80.5	87.9	81.0	**89.6**	83.53
Subspace kNN	70.9	88.4	82.0	85.7	79.5	88.7	80.3	**89.5**	83.13
RUSBoosted Trees	55.8	62.3	72.7	**81.1**	55.9	60.5	50.8	65.6	63.09
Average	68,6	82.72	82.12	86.12	76.62	83.98	75.74	**86.00**	

Table 4
3D Emotion Recognition Approaches.

Author	Dataset	Emotional State	Accuracy Rate	Method	Classifier
Liu and Sourina [11]	IADS & DEAP	High/Low Arousal & High/Low Dominance & 4 levels Valence Dimension Combinations	Min 23.2, 9nd Level Max100, 2nd Level	Statistical Features & Fractal Dimensions based features	Support Vector Machine
Verma and Tiwary [63]	DEAP	Valence Arousal Dominance	67.5 (Valence) 69.6 (Arousal) 65.1 (Dominance)	Multiresolution Analysis based multi-modality fusion (EEG & Video Features)	Multilayer Perceptron, Nearest Neighborhood, Support Vector Machine
Walter et. al [64]	Self-Dataset (IAPS)	PVLAHD NVHADD	70.1 (individual)	Statistical features, EMG, Peak-searching method, Blood Volume Pressure Statistical features, Galvanic Skin Response	Artificial Neural Network
Guendil et al. [18]	DEAP	Valence Arousal Dominance & Two Levels	73.43 (Valence) 72.65 (Arousal) 69.3 (Dominance)	Wavelet based features	Extreme Learning Machine

sis methods. To take multichannel interdependencies into account, data from all available channels are included in the feature extraction by using the MSST algorithm as opposed to the individual application of SST of each channel.

Our first observation is that the classification performances for all classifiers and emotion states were higher in the 3D emotion model than 2D model. This may be because the VAD parameters better define the emotional space than just VA parameters. Even though we expected to observe the effect/contribution of multichannel analysis, our 3D emotional domain classification results indicated that the performance using single channel SST, and MSST were highly similar for almost all classifiers and all emotion states. For the best classifiers, among all states the accurate prediction rate was the highest in NVLAHD and the lowest in PVLAHD whose values ranged from almost 75 to 93%. We observed that use of multivariate SST algorithm for all channels was significantly slower than SST application on each channel individually. However, when SST was applied to each channel separately and the results were combined to utilize all channel contributions the processing time was longer.

We compared our method to other 3D model studies where the dominance parameter is included, by using 4 classifier families and 20 different approaches and the comparison is provided in Table 4. It is shown in the performances that combining the arousal, valence and dominance dimensions to obtain eight different emotional states and utilizing SST and MSST in feature

extraction helped us achieve higher classification accuracies than most of the approaches in the table.

We should also note that using this database it was difficult to classify emotions with very high accuracies, because we think that the stimulant videos might have incited several emotions simultaneously. In this study we have just used multichannel EEG signals. In future studies we consider using other bio-signals in the feature extraction process. We believe that the MSST applications will also be improved to obtain better prediction accuracies. Additionally, there are some emotions which can be mixed among different languages such as happy and joy. In future studies, tools that make emotions more expressible can be facilitated for emotion state prediction. Finally, a more comprehensive database with various bio-signals could be developed.

Acknowledgment

Aydin Akan was supported by Izmir Katip Celebi University Scientific Research Projects Coordination Unit: Project number 2017-ÖNAP–MÜMF-0002.

References

[1] L.M.S. Morillo, J.A. Alvarez-Garcia, L. Gonzalez-Abril, J.A.O. Ramírez, Discrete classification technique applied to TV advertisements liking recognition system based on low-cost EEG headsets, Biomed. Eng. Online 15 (1) (2016) 197–218.
[2] Y. Liu, O. Sourina, M.K. Nyuyen, Real time EEG based emotion recognition and its applications, Trans. Comput. Sci. XII (2011) 256–277.
[3] A. Mert, A. Akan, Emotion recognition from EEG signals by using multivariate empirical mode decomposition, Pattern Anal. Appl. (2018) 81–89.
[4] R. Plutchik, Emotion: A Psychoevolutionary Synthesis, Harper and Row, New York, 1980.
[5] P. Ekman, W.V. Friesen, M. O'Sullivan, A. Chan, I. Diacoyanni-Tarlatzis, K. Heider, P.E. Ricci-Bitti, Universals and cultural differences in the judgments of facial expressions of emotion, J. Pers. Soc. 53 (4) (1987) 712–717.
[6] J.A. Russell, A circumplex model of affect, J. Pers. Soc. Pschol. 39 (1980) 1161–1178.
[7] A. Mehrabian, J.A. Russell, An Approach to Environmental Psychology, MIT Press, Cambridge, MA, 1974.
[8] Y. Liu, O. Sourina, EEG-based dominance level recognition for emotion-enabled interaction, IEEE International Conference on Multimedia and Expo (2012).
[9] A.G. Aguinaga, A.L. Ramirez, M.R.B. Flores, Classification model of arousal and valence mental states by EEG signals analysis and Brodman correlations, Int. J. Adv. Comput. Sci. Appl. 6 (6) (2015).
[10] Y. Liu, O. Sourina, EEG databases for emotion recognition, International Conference on Cyberworlds (2013).
[11] Y. Liu, O. Sourina, Real time fractal based valence level recognition from EEG, Trans. Comput. Sci. (2013) 101–120.
[12] Y. Liu, O. Sourina, EEG-based subject dependent emotion recognition algorithm using fractal dimension, IEEE International Conference on Systems,Man, and Cybernetics (2014).
[13] Y. Liu, O. Sourina, M.R. Hafiyyandi, EEG-based emotion-adaptive advertising, Humaine Association Conference on Affective Computing and Intelligent Interaction (2013).
[14] G.K. Verma, U.S. Tiwary, Multimodal fusion framework: a multiresolution appraoch for emtotion classification and recognition from physiological signals, Neuroimage 102 (2014) 162–172.
[15] G.K. Verma, U.S. Tiwary, Affect representation and recognition in 3D continuous valence-arousal-dominance space, Multimed. Tools Appl. (2016) 1–25.
[16] S. Walter, J. Kim, D. Hrabal, S.C. Crawcour, H. Kessler, H.C. Traue, Transsituational individual-specific biopsychological classification of emotions, IEEE Trans. Syst. Man Cyber. Syst. 43 (4) (2013), July.
[17] M. Wyczesany, T.S. Ligeza, Towards a constructionist approach to emotions: verification of the three-dimensional model of affect with EEG-independent component analysis, Exp. Brain Res. 233 (3) (2015) 723–733.
[18] Z. Guendil, Z. Lachiri, C. Maaoui, Computational framework for emotional VAD prediction using regularized Extreme Learning Machine, Int. J. Multimed. Inf. Retrieval 6 (3) (2017) 251–261.
[19] R. Jenke, A. Peer, M. Buss, Feature extraction and selection for emotion recognition from EEG, IEEE Trans. Affect. Comput. 5 (3) (2014).
[20] I. Daubechies, J. Lu, H.T. Wu, Synchrosqueezed wavelet transforms: an empirical mode decompositionlike tool, Appl. Comput. Harmon. Anal. (2011) 243–261.
[21] N.E. Huang, Z. Shen, S.R. Long, M.C. Wu, H.H. Shih, Q. Zheng, N.C. Yen, The emprical mode decomposition and the Hilbert spectrum for nonlinear and non-stationary time series anaylsis, Proc. R. Soc. Lond. 454 (1998) 903–995.
[22] D. Ur Rehman, D.P. Mandic, Filter bank property of multivariate empirical mode decomposition, IEEE Trans. Signal Process. 59 (2011) 2421–2426.
[23] A. Khasnobish, S. Bhattacharya, G. Singh, A. Jati, A. Konar, D.N. Tibarewala, R. Janarthanan, The role of emprical mode decomposıtıon on emotion classification using stimulated EEG signals, Adv. Comput. Inf. Technol. 178 (2013) 55–62.
[24] A.S. Guzman, M. Fischer, U. Heute, G. Schmidt, Real-time empirical mode decomposition for EEG signal enhancement, Signal Processing Conference (EUSIPCO), 2013 Proceedings of the 21st European (2013).
[25] C. Shahnaz, S.B. Masud, S.M.S. Hasan, Emotion recognition based on wavelet analysis of empirical mode decomposed EEG signals responsive to music videos, IEEE Region 10 Conference (TENCON) (2016).
[26] A.K. Maity, R. Pratihar, A. Mitra, S. Dey, V. Agrawal, S. Sanyal, A. Banerjee, R. Sengupta, D. Ghosh, Multifractal Detrended Fluctuation Analysis of alpha and theta EEG rhythms with musical stimuli, Chaos Solitons Fractals 81 (Part A) (2015) 52–67, December.
[27] N. Zhuang, Y. Zeng, L. Tong, C. Zhang, H. Zhang, B. Yan, Emotion eecognition from EEG Signals using multidimensional information in EMD domain, Biomed Res. Int. 2017 (2017) 1–9.
[28] H. Xu, Towards Automated Recognition of Human Emotion Using EEG, University of Toronto, Toronto, Canada, 2012.
[29] Y. Tonoyan, D. Looney, D.P. Mandic, M.M. Van Hulle, Discriminating multiple emotional states from EEG using a data-adaptive, multiscale information-theoretic approach, Int. J. Neural Syst. 26 (2016) 1650005, 15 pages.
[30] C. Guitton, Emotions Estimation From EEG Recordings, Imperial Collage of Science, Technology & Medicine Department of Electrical& Electronic Engineering, London, 2010.
[31] H. Xu, K.N. Plataniotis, Application of multivariate emprical mode decomposition in eeg signals for subject independent affective states classification, Int. J. Commun. 9 (2015) 91–97.
[32] N. Ur Rahman, C. Park, N.E. Huang, D.P. Mandic, EMD via MEMD: multivariate noise aided computation of standard EMD, Adv. Adapt. Data Anal. 5 (2013) 1350007, 25 pages.
[33] Z. Huang, J. Zhang, T. Zhao, Y. Sun, Synchrosqueezing S-Transform and its application in seismic spectral decomposition, IEEE Trans. Geosci. Remote. Sens. 54 (2) (2016) 817–825.
[34] H.-T. Wu, Adaptive Analysis of Complex Data Sets, Princeton University, New Jersey, USA, 2019.
[35] A. Ahrabian, D. Looney, L. Stanković, D.P. Mandic, Synchrosqueezing-based time frequency analysis of multivariate data, Signal Process. (2015) 331–341.
[36] J.M. Lilly, S.C. Olhede, Wavelet ridge estimation of jointly modulated multivariate oscillations, Conference Record of the Forty Third Asilomar Conference on Signals, Systems and Computers (2009).
[37] J.M. Lilly, S.C. Olhede, Analysis of modulated multivariate oscillations, IEEE Trans. Signal Process. (2) (2012) 600–612.
[38] S. Olhede, A.T. Walden, The Hilbert spectrum via wavelet projections, R. Soc. 460 (2044) (2004) 955–975.
[39] S. Koelstra, C. Mühl, M. Soleymani, J.S. Lee, A. Yazdani, T. Ebrahimi, I. Patras, DEAP: a database for emotion analysis; using physiological signals, IEEE Trans. Affect. Comput. 3 (2012) 18–31.
[40] http://www.gtec.at, G-TEC Medical Engineering.
[41] M. Sreeshakthy, J. Preethi, A. Dhilipan, A survey on emotion classification from eeg signal using various techniques and performance analysis, I.J. Inf. Technol. Comput. Sci. 12 (2016) 19–26.
[42] T.M. Mitchell, Machine Learning, McGraw-Hill, Boston, 1997.
[43] J.F. Bell, Application of classification trees to habitat preference of uphand birds, J. Appl. Stat. 23 (1999) 349–359.
[44] R.O. Duda, P.E. Hart, D.G. Stork, Pattern Classification, 2nd ed., John Wiley & Sons, New York, 2000.
[45] S. Lessmann, B. Baesens, H.V. Seow, L.C. Thomas, Benchmarking state-of-the-art classification algorithms for credit scoring: an update of research, Eur. J. Oper. Res. 237 (1) (2015) 124–136.
[46] S. Finlay, Multiple Classifier architectures and their application to credit risk assessment, Eur. J. Oper. Res. 210 (2011) 368–378.
[47] G. Paleologo, A. Elisseeff, G. Antonini, Subagging for credit scoring models, Eur. J. Oper. Res. 201 (2019), pp. 490-490499, 210.
[48] C.M. Bishop, Pattern Recognition and Machine Learning, Springer, 2006.
[49] A. Ben-hur, J. Weston, A user's guide to support vector machines, in: Data Mining Techniques for the Life Sciences, 2010, pp. 223–239.
[50] Soraia M. Alarcao, Manuel J. Fonseca, Emotions recognition using EEG signals: a survey, IEEE Trans. Affect. Comput. 99 (2017), 1–1.
[51] R. Jenke, A. Peer, M. Buss, Effect-size-based electrode and feature selection for emotion recognition from EEG, IEEE International Conference on Acoustics, Speech and Signal Processing (ICASSP) (2013).
[52] J. Zhang, M. Chen, S. Zhao, S. Hu, Z. Shi, Y. Cao, ReliefF-based EEG sensor selection methods for emotion recognition, Sensors 1558 (2016) 16.
[53] S. Hatamikia, A.M. Nasrabadi, Common spatial pattern method for channel reduction in EEG based emotion recognition, Modares J. Electr. Eng. 13 (1) (2016) 31–43.
[54] N. Zhuang, Y. Zeng, K. Yang, C. Zhang, L. Tong, B. Yan, Investigating patterns for self-induced emotion recognition from EEG signals, Sensors 18 (841) (2018) 1–22.
[55] N. Zhuang, Y. Zeng, L. Tong, C. Zhang, H. Zhang, B. Yan, Emotion recognition from EEG signals using multidimensional information in EMD domain, Biomed Res. Int. 2017 (2017) 1–9.

[56] M.S. Ozerdem, H. Polat, Emotion recognition based on EEG features in movie clips with channel selection, Brain Inf. 4 (4) (2017) 241–252.
[57] S.K. Hadjidimitriou, L. Hadjileontiadis, Towards an EEG-based recognition of music liking using time-frequency analysis, IEEE Trans. Biomed. Eng. 59 (12) (2012) 3498–3510.
[58] Y.-P. Lin, C.-H. Wang, T.-P. Jung, T.-L. Wu, S.-H. Jeng, J.-R. Duann, J.-H. Chen, EEG-based emotion recognition in music listening, IEEE Trans. Biomed. Eng. 57 (7) (2010) 1798–1806.
[59] E. Kroupi, A. Yazdani, T. Ebrahimi, EEG correlates of different emotional states elicited during watching music videos, Affect. Comput. Intell. Inter. Lect. Notes Comput. Sci. 6975 (2011) 457–466.
[60] V. Rozgić, S.N. Vitaladevuni, R. Prasad, Robust EEG emotion classification using segment level decision fusion, IEEE International Conference on Acoustics, Speech and Signal Processing (ICASSP) (2013).
[61] S. Ayhan, Ş. Erdoğmuş, Destek Vektör Makineleriyle Sınıflandırma Problemlerinin Çözümü için Çekirdek Fonksiyonu Seçimi, Eskişehir Osmangazi Üniversitesi IIBF Dergisi, 2014, pp. 175–201.
[62] A. Jović, K. Brkić, N. Bogunović, Decision Tree Ensembles in Biomedical Time-series Classification, Pattern Recognition. DAGM/OAGM 2012, Lecture Notes in Computer Science, Berlin, Heidelberg, 2012.
[63] G.K. Verma, U.S. Tiwary, Affect Representations and recogniiton in 3D continuous valence-arousal-dominance space, Multimed. Tools Appl. 76 (2) (2017) 2159–2183.
[64] S. Walter, J. Kim, D. Hrabal, S.C. Crawcour, H. Kessler, H.C. Traue, Transsituational individual-specific biopsychological classification of emotions, IEEE Trans. Syst. Man Cyber. Syst. 43 (4) (2013).